



Nonlinear laser lithography to control surface properties of stainless steel

L. Orazi ^{a,*}, Ia. Gnilitzky ^a, I. Pavlov ^b, A.P. Serro ^{c,d}, S. Ilday ^b, F.O. Ilday ^{b,e}



^a Department of Science and Methods for Engineering, University of Modena and Reggio Emilia, Italy

^b Department of Physics, Bilkent University, Turkey

^c Centro de Química Estrutural, Instituto Superior Técnico, University of Lisbon, Portugal

^d Centro de investigação Interdisciplinar Egas Moniz, Instituto Superior de Ciências da Saúde Egas Moniz, Portugal

^e Department of Electrical and Electronics Engineering, Bilkent University, Turkey

Submitted by Prof. Marco Santochi (1)

ARTICLE INFO

Keywords:

Laser micro machining
Nanostructure
Surface modification

ABSTRACT

In the present work a novel method to improve the surface properties of stainless steel is presented and discussed. The method, based on the use of a high repetition rate femtosecond Yb fibre laser, permits generation of highly reproducible, robust, uniform and periodic nanoscale structures over a large surface area. The technique is characterized by high productivity, which, in its most simple form, does not require special environmental conditioning. Surface morphology is scrutinized through SEM and AFM analyses and wettability behaviour is investigated by means of the sessile drop method using distilled–deionized water. It is shown that optimization of process parameters promotes anisotropic wetting behaviour of the material surface.

© 2015 CIRP.

1. Introduction

Control of the wettability behaviour of a stainless steel surface can be of great interest for several applications. This class of materials is known to be largely used by food, dairy and pharmaceutical production systems owing to their intrinsic chemical stability and strong resistance to oxidation that permit them to be safely cleaned and disinfected by using several chemical agents.

In all these applications, control of surface wettability can be of great interest, as it can lead to shorter cleaning and flushing times, less organic residuals in pipes and components and minimal retention of chemical agents on the surface. Several methods were developed to control the wetting behaviour of stainless steel. A significant part of them investigated the effect of chemical composition of the surface, by modifying it via surface coatings or through reaction of the base material with other chemical agents. In [1] several approaches were attempted, namely implantation of different ions (e.g. SiF_3^+ and MoS_2^{2+}) into stainless steel; coating the surface with diamond-like carbon (DLC) via sputtering; plasma chemical vapour deposition (PECVD) of DLC, DLC–Si–O coating onto the surface and treating the surface by autocatalytic Ni–P–PTFE and silica coating. In [2] and [3], the authors carried out electrolytic in-process dressing (ELID) grinding to generate a mirror-quality surface on ferritic stainless steel for surgical applications. This method is used to functionalize the surface by varying the type and quantity of abrasive materials or

the operating temperature in order to induce different wettability behaviour. Some of the above methods are expensive, complicated and time consuming; others involve chemical treatments and weak coatings that are generally evanescent or fragile. Use of methods that only change the surface morphology/topography could be the safer choice if chemical stability is critical for an application, where no surface contaminations are desired.

Two different recent examples can be found in [4,5] based respectively on a vibration assisted machining method and on the use of a nanosecond UV laser.

It is well known that femtosecond lasers can generate regular structures on a material's surface called laser induced periodic surface structures (LIPSS), of which a recent example can be found in [6]. This principle can be applied to obtain hydrophobic surfaces as investigated in [7,8], where stainless steel and titanium alloys were treated with a Ti:Sapphire femtosecond laser and eventually silanized in a low vacuum chamber. Although the results are appealing, the methods cannot be easily scaled for mass production due to the low production rate which is a consequence of the characteristics of the lasers employed: high pulse energies and low pulse frequencies and scanning speeds.

Recently, a technique called nonlinear laser lithography (NLL) has been introduced which permits production of highly uniform nanostructures on large surface areas with an elevated production rate. This technique is based on the use of a high repetition rate, well-focused femtosecond laser with pulse energy in the order of nanojoules. A comprehensive physical model of the process has been presented in [9].

In this work, the NLL technique is employed to modify the surface topography of stainless steel and control its wettability behaviour due to its unique features over other surface modification methods

* Corresponding author.

E-mail address: leonardo.orazi@unimore.it (L. Orazi).

such as controlled thermal penetration, chemical cleanness and remote non-contact processing.

2. Experimental setup

The material under study was a commonly used AISI 316L stainless steel that is subjected to a low temperature carburizing (LTC) process where the elevated carbon content in the $30 \pm 2 \mu\text{m}$ treated depth strongly increases the surface hardness from 200 to 1200 Vickers. A cross-section image of the material under metallographic study is shown in Fig. 1.

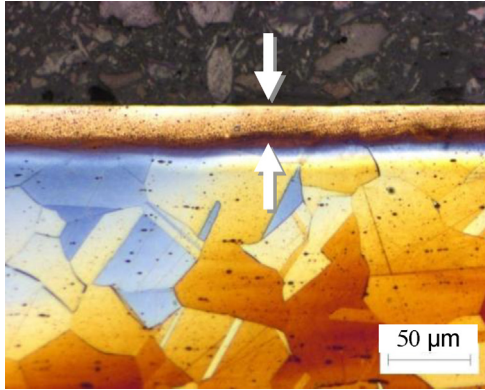


Fig. 1. A cross-section image of AISI LTC under metallographic study. The treated zone of about $30 \mu\text{m}$ on the surface is indicated by arrows.

The NLL treatments were conducted by using a custom-built Ytterbium fibre laser with a wavelength centred at $1037 \pm 8 \text{ nm}$. The laser beam was linearly polarized and guided onto the material surface with a galvanometric scanning head focused by a 56 mm focal length F-theta lens.

The surface of the material was first polished and lapped with diamond paste then areas of $5 \text{ mm} \times 5 \text{ mm}$ were NLL treated to form periodic nanostructures.

Coding of the specimens along with the experimental variables such as the polarization angle of the laser beam (θ_p), the angle between the polarization plane and the scanning direction, and pulse energies are given in Table 1. Other parameters were kept constant such as the pulse duration (270 fs) repetition rate (200 kHz), spot diameter ($6 \mu\text{m}$), scanning speed (100 mm/s) and step between the scanned lines ($2 \mu\text{m}$), which resulted in a high overlapping between the laser pulses, a condition necessary to generate uniform, periodic surface structures. The process production rate was $0.5 \text{ cm}^2/\text{min}$.

Table 1
Coding of the specimens and experimental variables.

Coding of the specimen	Polarization angle θ_p ($^\circ$)	Pulse energy (nJ)
PPA	0	160
PPB	0	170
PPC	0	180
PTA	90	160
PTB	90	170
PTC	90	180

PP coding denotes tests in which the polarization plane is parallel to the scanning direction, whereas PT coding denotes those in which the polarization plane is perpendicular to the scanning direction.

The surface morphology of the specimens was observed through Variable Pressure Scanning Electron Microscopy coupled with energy dispersive spectroscopy operated in secondary electrons imaging mode. Three-dimensional images of the surfaces were obtained from stereoscopic pairs of images acquired at tilting

angles of 0 and 45° . Surface roughness was measured by using an atomic force microscope (AFM) in non-contact optical mode.

The wettability of the surfaces was determined through the measurement of distilled and deionized (DD) water contact angles by the sessile drop method. Drops of $\approx 2\text{--}4 \mu\text{L}$ were generated with a micrometric syringe and deposited on the substrate surfaces, inside a chamber previously saturated with water. Drop images were acquired at pre-defined intervals during 2000s, with the system composed of a video camera connected to a microscope and a frame grabber to sequentially capture the drop profile. Longer measurements were not done, since evaporation of the liquid can be a problem for long times. Each image was then analyzed by software to evaluate the contact angle. The measurements were done at 25°C . At least 4 drops were generated and measured for each specimen.

3. Results and discussions

3.1. Morphological results

Fig. 2 presents a representative SEM image of a PP-coded specimen where the polarization plane is parallel to the scanning direction. As can be seen from the figure, formation of a quasi-regular linear pattern is evident with all the basic aspects of NLL present: the coherent propagation of structures along the surface that are obtained by scanning the laser beam with a small diameter [9]. In our case the basic mechanism of generation could be the interaction of the incident laser beam with surface plasmon polaritons (SPPs) instead of wave scattered in the surface [10].

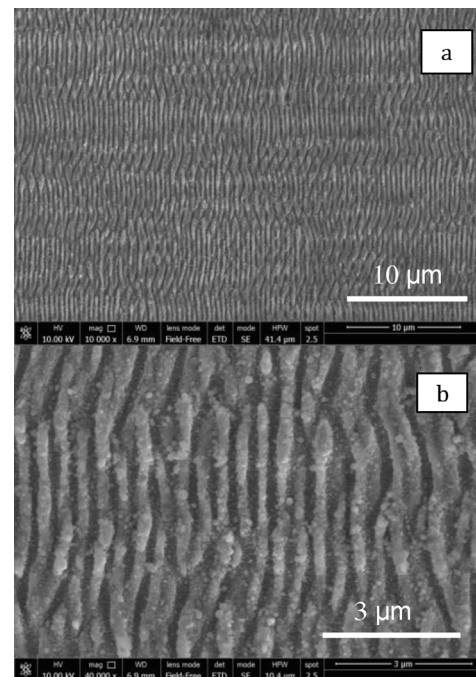


Fig. 2. SEM images of the specimen coded as PPC, where the scanning direction and the polarization plane are parallel to each other: (a) a large area image, and (b) the focused image taken in higher magnification.

The periodicity of LSFL was measured as $380 \pm 50 \text{ nm}$. AFM analyses indicated that the width and the height of the ripples are $320 \pm 40 \text{ nm}$ and $420 \pm 30 \text{ nm}$, respectively.

Image in Fig. 2b shows the presence of ripples of high spatial frequency LIPSS (HSFL) inside the valleys between periodic structures. A nanostructure parallel to the polarization direction is evident with a period significantly smaller than the laser wavelength and in the order of $77 \pm 20 \text{ nm}$.

Fig. 3 shows the AFM mapping of the specimen coded as PTB, where the scanning direction and the polarization plane are

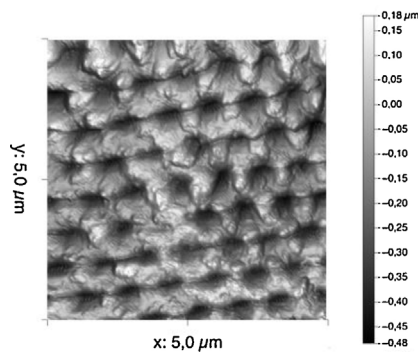


Fig. 3. AFM maps of PTB treatment with a quasi-hexagonal structure clearly visible.

perpendicular to each other. The nanostructures are clearly different with respect to the specimen coded as PPC, with quasi-hexagonal structures in three principal directions that are mutually oriented at 60° to one another. It seems like two small ripples are periodically joined in a bigger ripple. The period between these double ripples was measured as 790 ± 30 nm, while the period between the smaller ripples was measured as 350 ± 50 nm, almost half of the period of double ripples.

The quasi-hexagonal structures were already obtained and observed in previous studies, where the structures were produced by scanning the surface with a circularly polarized laser beam or by using double scans with two orthogonal polarizations [11]. In our case it is possible that the galvoscaner perturbs the polarization state to elliptical depending on the scanning speed and initial polarization. The structures are clearly evident in SEM images shown in Fig. 4, where they are taken from a 45° tilted specimen. Fig. 4b depicts the high-resolution image showing the joint of two ripples.

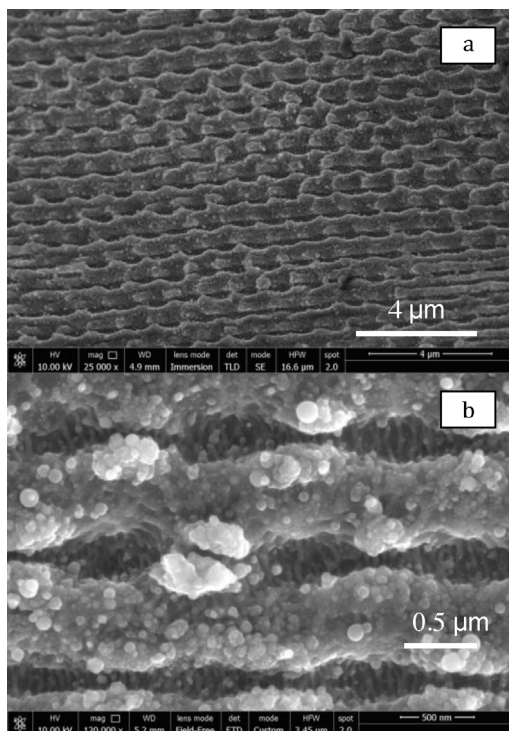


Fig. 4. SEM images of the specimen coded as PTB, where the scanning direction and the polarization plane are perpendicular to each other: (a) a large area image, and (b) the focused image taken at a higher magnification.

Roughness data were measured by analysing the AFM maps of the different treatments and are presented in Table 2. The untreated surface is indicated as UNT, presenting very high values of high order statistical moments. This is probably due to noise in the AFM images, while the other indicators R_a , R_q and the relative

Table 2
Roughness data as obtained from AFM analysis.

	Sa (nm)	Sq (nm)	Skew (-)	Kurtosis (-)	Relative area (-)
PPA	79.7	103.1	0.290	0.765	2.02
PPB	86.7	111.8	0.437	0.919	2.16
PPC	98.4	125.9	0.271	0.811	1.66
PTA	52.0	66.3	0.411	0.492	1.52
PTB	61.9	79.0	0.195	0.509	1.41
PTC	87.0	110.9	0.303	0.712	1.87
UNT	11.9	16.7	2.284	14.106	1.02

area are as expected. PP treatments present a moderate increase in all roughness indicators with respect to PT treatments.

3.2. EDS analysis

Chemical compositions of the untreated specimen and NLL-treated specimen coded as PTB were analyzed through an EDS probe and the results are given in Tables 3 and 4, respectively. Although there is an uncertainty on low atomic number elements like carbon, the values obtained for the untreated specimen are in a good agreement with the nominal chemical composition of an AISI 316L that is subjected to a low temperature carburizing treatment. On the other hand, Table 4 shows that when the surface is NLL-treated, it is possibly oxidized as a result of laser-material interaction in the atmospheric conditions.

Table 3
Results of the EDS analysis of the untreated specimen.

Element	Series	wt. (%)	Norm. wt. (%)	Norm. at. (%)	3σ err. in wt. (%)
C	K	3.59	4.32	17.31	3.58
Si	K	0.29	0.34	0.59	0.15
Cr	K	12.84	15.46	14.31	1.16
Mn	K	2.66	3.20	2.81	0.36
Fe	K	54.79	65.96	56.85	4.40
Ni	K	7.22	8.69	7.12	0.76
Mo	L	1.68	2.02	1.01	0.33
Sum		83.07	100.00	100.00	

Table 4
Results of the EDS analysis of the specimen coded as PTB.

Element	Series	wt. (%)	Norm. wt. (%)	Norm. at. (%)	3σ err. in wt. (%)
C	K	5.80	6.57	23.95	4.94
O	K	1.14	1.30	3.54	1.22
Si	K	0.39	0.44	0.68	0.17
Cr	K	12.82	14.52	12.22	1.15
Mn	K	2.53	2.87	2.28	0.35
Fe	K	55.64	63.01	49.38	4.47
Ni	K	8.48	9.60	7.16	0.87
Mo	L	1.51	1.71	0.78	0.31
Sum		88.32	100.00	100.00	

3.3. Wettability analysis

Wettability tests with DD water were conducted through the sessile drop method on both types of surfaces.

Measurements were performed in two directions: parallel and perpendicular to LIPPS (Fig. 5), to evaluate the effect of the NLL treatments on anisotropic wettability measured as the difference between the contacts angles observed in those directions.

The results are presented in Figs. 6 and 7 for the specimens coded as PPC and PTB, respectively. Data obtained for the untreated specimen are included for the purpose of comparison. Results scattering is shown as light coloured bands.

Both NLL treated surfaces present an appreciable hydrophobicity. This is coherent with earlier studies, where femtosecond laser irradiation is used to treat stainless steel surfaces [12–14]. Depending on the experimental conditions, some of them have

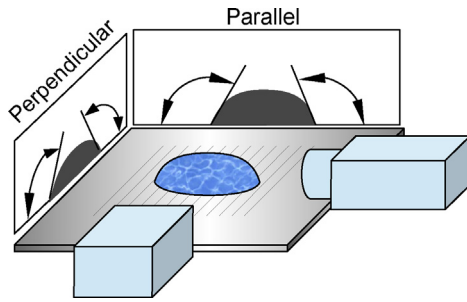


Fig. 5. Schematic representation of the contact angle measurement in parallel and perpendicular directions.

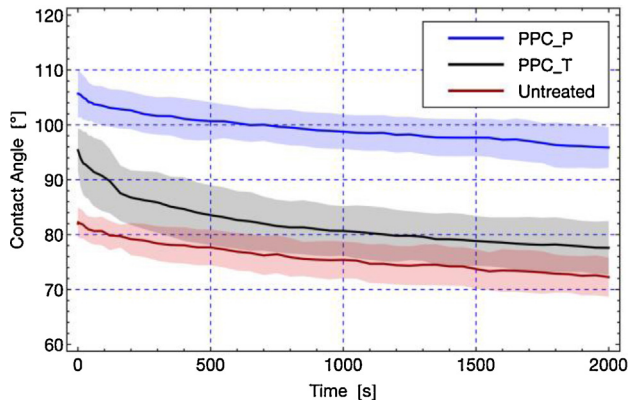


Fig. 6. Evolution of the water contact angles with time for the specimen coded as PPC. PPC_P represents the measurements performed when the contact angle is in a plane perpendicular to the LIPPS direction, while PPC_T represents the measurements performed when the contact angle is in a plane parallel to the LIPPS direction as indicated in Fig. 5.

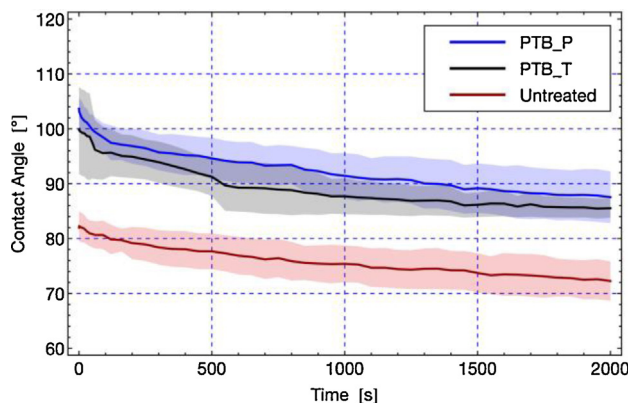


Fig. 7. Evolution of the water contact angles with time for the specimen coded as PTB. PTB_P represents the measurements performed when the contact angle is in a plane perpendicular to the LIPPS direction, while PTB_T represents the measurements performed when the contact angle is in a plane parallel to the LIPPS direction as indicated in Fig. 5.

managed to achieve super-hydrophobic surfaces. Obviously, the increase in hydrophobicity may be attributed not only to changes in roughness and topography as predicted by the Wenzel model [15] but also due to the oxidation induced by the laser treatment as evidenced by data from Table 4.

The main difference in the wettability behaviour of the two surfaces is related with the degree of anisotropy. As expected, contact angles observed perpendicularly to the LIPPS direction are smaller than those observed in the parallel direction because grooves drive water by capillary force. The difference between the contact angles in the two directions, however, is more pronounced in PPC surfaces (Fig. 6). From the morphological analysis carried

out above, it was concluded that NLL treatments led to a strong linearly structured texture on PP surfaces and a more isotropic (quasi-hexagonal) structure on PT surfaces. This is reflected by the wettability results. Moreover, as observed by other researchers [16], the contact angle anisotropy is strongly correlated to the surface arithmetic mean roughness (Sa); rougher samples (as is the case of PP, see Table 2) show larger wetting anisotropy than the smoother ones. The average increase in contact angle measured on the entire set of wettability tests performed is 15.8° while the average anisotropy calculated as the difference between the contact angle in the two directions appears to be 8.4° for PP test conditions and 5.8° for PT ones, respectively.

4. Conclusions

The NLL technique appears to be a very promising method for the control of the wettability properties of stainless steel. The presented setup permitted an increase in hydrophobicity by using a low power and not particularly expensive femtosecond laser. The process seems to be quite robust and repeatable also if conducted in open air, while it can be easily scaled to mass production by increasing power and scanning speed.

All the results confirm it is possible to increase the surface hydrophobicity with the possibility to tune, in a single pass treatment, the degree of anisotropy by varying the experimental conditions.

References

- [1] Santos O, Nylander T, Rosmaninho R, Rizzo G, Yiantsios S, Andritsos N, et al (2004) Modified Stainless Steel Surfaces Targeted to Reduce Fouling-Surface Characterization. *Journal of Food Engineering* 64:63–79.
- [2] Ohmori H, Katahira K, Komotori J, Mizutani M (2008) Functionalization of Stainless Steel Surface Through Mirror-Quality Finish Grinding. *CIRP Annals – Manufacturing Technology* 57(1):545–549.
- [3] Ohmori H, Katahira K, Komotori J, Akahane Y, Mizutani M, Naruse T (2009) Surface Generation of Superior Hydrophilicity for Surgical Steels by Specific Grinding Parameters. *CIRP Annals – Manufacturing Technology* 58(1):503–506.
- [4] Guo P, Lu Y, Ehmann KF, Cao J (2014) Generation of Hierarchical Microstructures for Anisotropic Wetting by Elliptical Vibration Cutting. *CIRP Annals – Manufacturing Technology* 63(1):553–556.
- [5] Chun D-M, Davaasuren G, Ngo C-V, Kim C-S, Lee G-Y, Ahn S-H (2014) Fabrication of Transparent Superhydrophobic Surface on Thermoplastic Polymer Using Laser Beam Machining and Compression Molding for Mass Production. *CIRP Annals – Manufacturing Technology* 63(1):525–528.
- [6] Romoli L, Rashed CAA, Lovicu G, Dini G, Tantussi F, Fuso F, Fiaschi M (2014) Ultrashort Pulsed Laser Drilling and Surface Structuring of Microholes in Stainless Steels. *CIRP Annals – Manufacturing Technology* 63(1):229–232.
- [7] Wu B, Zhou M, Li J, Ye X, Li G, Cai L (2009) Superhydrophobic Surfaces Fabricated by Microstructuring of Stainless Steel Using a Femtosecond Laser. *Applied Surface Science* 256(1):61–66.
- [8] Bizi-Bandoki P, Benayoun S, Valette S, Beaugiraud B, Audouard E (2011) Modifications of Roughness and Wettability Properties of Metals Induced by Femtosecond Laser Treatment. *Applied Surface Science* 257(12):5213–5218.
- [9] Öktem B, Pavlov I, Ilday S, Kalaycıoğlu H, Rybak A, Yavaş S, Erdoğan M, Ilday F.Ö. (2013) Nonlinear Laser Lithography for Indefinitely Large-Area Nanostructuring with Femtosecond Pulses. *Nature Photonics* 7(11):897–901.
- [10] Derrien TJ-Y, Torres R, Sarnet T, Sentis M, Itina TE (2012) Temperature dependence of laser-induced micro/nanostructures for femtosecond laser irradiation of silicon. *Appl Surf Sci* 258:9487.
- [11] Anzolin G, Gardelein A, Jofre M, Molina-Terizza G, Mitchell MW (2010) Polarization Change Induced by a Galvanometric Optical Scanner. *Journal Optical Society of America* 27(9):1946–1952.
- [12] Liang C, Li B, Wang H, Li B, Yang J, Zhou L, Li H, Wang X, Li C (2014) Preparation of Hydrophobic and Oleophilic Surface of 316 L Stainless Steel by Femtosecond Laser Irradiation in Water. *Journal of Dispersion Science and Technology* 35:1345–1350.
- [13] Kam DH, Bhattacharya S, Mazumder J (2012) Control of the Wetting Properties of an AISI 316L Stainless Steel Surface by Femtosecond Laser-Induced Surface Modification. *Journal of Micromechanics and Microengineering* 22:105019–105025.
- [14] Oberringer M, Akman E, Lee J, Metzger W, Akkan CK, Kacar E, et al (2013) Reduced Myofibroblast Differentiation on Femtosecond Laser Treated 316L. *Materials Science and Engineering C* 33:901–908.
- [15] Wenzel RN (1936) Resistance of Solid Surfaces to Wetting by Water. *Industrial and Engineering Chemistry* 28:988–994.
- [16] Calvimontes A, Mauer mann M, Bellmann C (2012) Topographical Anisotropy and Wetting of Ground Stainless Steel Surfaces. *Materials* 5:2773–2782.